PHYSICAL REVIEW B, VOLUME 63, 201202(R)

Magnetism of chalcopyrite semiconductors: $Cd_{1-x}Mn_xGeP_2$

Yu-Jun Zhao, W. T. Geng, and A. J. Freeman
Department of Physics & Astronomy, Northwestern University, Evanston, Illinois 60208

T. Oguchi
Department of Quantum Matter, ADSM, Hiroshima University, Higashihiroshima 739-8526, Japan
(Received 21 February 2001; published 24 April 2001)

The recently reported room-temperature ferromagnetism in $Cd_{1-x}Mn_xGeP_2$ was investigated for $x=1.0$, 0.5, and 0.25 by the local density first-principles full-potential linearized augmented plane wave (FLAPW) and DMOL^3 methods within both local-density approximation (LDA) and generalized gradient approximation (GGA). We find that the total energy of the antiferromagnetic (AFM) state is lower than the corresponding ferromagnetic (FM) state for all x studied. The GGA gives a better description of magnetic properties than LDA mainly due to its better prediction of structure, particularly for high Mn concentrations. The total spin moment of $Cd_{1-x}Mn_xGeP_2$ is $\sim 5.0\mu_B$ per Mn atom. The FM alignment between Mn and P increases the total energy of the Mn-Mn FM coupling and makes the AFM ordering preferable.

DOI: 10.1103/PhysRevB.63.201202 PACS number(s): 75.50.Pp, 75.30.Hx

The discovery of ferromagnetism (FM) in III-V semiconductors such as (Ga,Mn)As (Refs. 1 and 2) and the successful control of spin coherence of electrons injected from a magnetic semiconductor into a nonmagnetic semiconductor suggests the possibility of harnessing both charge and spin for new functionalities.[3] While these developments hold considerable promise, in principle, the limiting factor that represents a serious bottleneck for their practical spintronic applications is the fact that both the observed FM and the attractive injection phenomena are essentially limited to low temperature. This bottleneck clearly arises from the specific properties of the magnetic semiconductor materials that are currently available, which so far have been limited primarily to III-V based alloys containing Mn ions.[4]

Very recently, Medvedkin *et al.*[5] incorporated high Mn concentrations into the surface region of a II-IV-V_2 type chalcopyrite semiconductor $CdGeP_2$ by vacuum deposition of Mn on the single-crystal surface followed by a solid phase reaction at elevated temperature. Now, the chalcopyrite differs from the zinc-blende crystal structure by a doubling of the unit cell along a fourfold axes, rendering the system body-centered tetragonal. The expected special advantage of these systems is that Mn can readily be substituted for II cations, as has been demonstrated for $II_{1-x}Mn_xIV$ alloys with x up to 1.0 without the formation of structural defects, owing to the natural tendency of Mn to adopt a $+2$ state. An important finding reported by Medvedkin *et al.* is the room-temperature ferromagnetism in highly doped $Cd_{1-x}Mn_xGeP_2$, which constitutes a tremendous improvement from the T_C of 110 K found in $Ga_{1-x}Mn_xAs$ for $x=5.3\%$. Also, their photoluminescence spectrum at 20 K shows a peak around 3.2 eV, from which they proposed a Mn-induced enhancement of the energy gap of $CdGeP_2$ ($E_g=1.83$ eV). This is quite different from the III-V alloys, in which Mn is known to reduce the band gap.

In order to understand the magnetic interaction in chalcopyrite semiconductors, we investigated $Cd_{1-x}Mn_xGeP_2$ with both the full-potential linearized augmented plane-wave[6] (FLAPW) and DMOL^3 methods.[7] We find that the antiferromagnetic (AFM) state has a lower total energy than the FM state and that Mn doping does not enlarge the energy gap in $Cd_{1-x}Mn_xGeP_2$ systems for $x=0.25$, 0.5, and 1.0.

DMOL^3, i.e., density functional theory (DFT) for molecules and three-dimensional periodic solids,[7] uses fast convergent three-dimensional numerical integrations to calculate the matrix elements occurring in the Ritz variational method.[8] The localized numerical linear combination of atomic orbital basis sets are designed to give a maximum accuracy for a given basis set size.[8] DMOL^3 has been successfully applied to band-structure calculations of insulating and metallic solids[7] and the complex structure of the $BaTiO_3$ grain boundary.[9] In this work, a double set of numerical valence functions with the local basis cutoff R_c of 9.0 a.u is employed. We found that the structure and magnetic properties of $MnGeP_2$ undergo no remarkable changes if an extended numerical basis or r_c of 11.0 a.u. is adopted. The relativistic treatments for the atoms are done via a pseudopotential[10] acting on all electrons, including core, to get scalar relativistic corrections for the relevant valence orbitals. Both the local-density approximation (LDA) functional of Perdew-Wang[11], and the generalized gradient approximation (GGA) functional of Perdew-Burke-Ernzerhof[12], are used to illustrate the dependence of our theoretical predictions on functional treatments. DMOL^3 is used to optimize the internal degrees of freedom of $Cd_{1-x}Mn_xGeP_2$ and the final results are checked by the highly reputed FLAPW method.

The well-known FLAPW method is one of the most accurate *ab initio* methods, in which there is no artificial shape approximation for the wave functions, charge density, and potential. For all atoms, the core states are treated fully relativistically and the valence states are treated semirelativistically (i.e., without spin-orbit coupling). Muffin-tin (MT) radii for Cd, Ge, and Mn are chosen as 2.30 a.u., and 1.8 a.u. is used for P. An energy cutoff of 9.0 Ry was employed for the augmented plane wave basis to describe the wave functions in the interstitial region, and a 49 Ry cutoff was used

for the star functions depicting the charge density and potential. Within the MT spheres, lattice harmonics with angular momentum l up to 8 were adopted. The LDA Hedin-Lundqvist functional[13] and the GGA functional with the same formula as in DMOL^3 [i.e, PBE (Ref. 12)] are employed based on the corresponding DMOL^3 optimized structure. As discussed below, the calculated Hellmann-Feynman forces are found to be well-balanced in the FLAPW calculation, which indicates that the DMOL^3 optimization is quite consistent with the FLAPW result.

Experimentally, the interplanar distances and lattice constants were found to decrease with Mn concentration in $Cd_{1-x}Mn_xGeP_2$ systems: $a=5.741$ Å $\rightarrow 5.710$ Å $\rightarrow 5.695$ Å in a series of $CdGeP_2 \rightarrow Cd_{1-x}Mn_xGeP_2 \rightarrow Cd_{1-y}Mn_yGeP_2$ $(x<y)$.[14] However, the detailed structural parameters of $Cd_{1-x}Mn_xGeP_2$ are not available. From our first-principles calculations, LDA and GGA give lattice constants with differences as large as $\sim 5\%$ for some systems, such as MnAs and GaAs.[15] Now, LDA gives a very good lattice constant for GaAs, but underestimates MnAs by about 5%. While GGA gives a much better (still underestimated by $\sim 1\%$) lattice constant for MnAs, it overestimates that of GaAs by $\sim 2\%$.[15]

Jaffe and Zunger proposed some effective rules for the lattice constant in ABC_2 chalcopyrite structures.[16] The nearest-neighbor anion-cation bond lengths are given by

$$R_{AC}=[u^2+(1+\eta^2)/16]^{1/2}a, \tag{1}$$

$$R_{BC}=\left[\left(u-\frac{1}{2}\right)^2+(1+\eta^2)/16\right]^{1/2}a, \tag{2}$$

where $\eta \equiv c/2a$. An enormous body of crystallographic studies has been directed at defining elemental radii that add up to the measured bond length $R_{ij} \simeq r_i + r_j$, which is referred to as the ''conservation of tetrahedral bonds'' (CTB).[16] The implication of this principle for the structural parameters a, η, and u of ABC_2 compounds is that these degrees of freedom would attain values that minimize simultaneously the difference between the actual anion-cation bond lengths R_{AC} and R_{BC} and the sums of elemental radii.[16]

Although R_{AC} and R_{BC} could be obtained from the elemental radii and the CTB rule, the a, u, and η could not obtained quantitatively unless another restriction is applied. Abrahams and Bernstein[17] proposed that the bond angles at the B atom in ABC_2 chalcopyrites would have the ideal tetrahedral values, which leads to

$$a^2=\frac{12\alpha^2}{2\beta+\alpha-[(2\beta+\alpha)^2-18\alpha^2]^{1/2}}, \tag{3}$$

$$\eta^2=\frac{8(\beta-\alpha)}{3\alpha^2}, \tag{4}$$

where $\alpha=R_{AC}^2-R_{BC}^2$, $\beta=R_{AC}^2+R_{BC}^2$.

The tetrahedral radii of Cd, Ge, and P obtained from Pauling's work are 1.48, 1.22, and 1.10 Å, respectively. Since it is already known that the bond lengths of MnS, MnSe, and MnTe in the tetrahedral structure are 2.432, 2.557, and 2.746 Å,[18] then the tetrahedral radius of Mn comes out to be $r_{Mn}=1.411\pm 0.019$ Å, if Pauling's tetrahedral radii are adopted for S, Se, and Te.[19] The Mn tetrahedral radius obtained by Yoder-Shorter *et al.*[18] is a little different from ours, since they used the covalent atomic radii of S, Se, and Te from van Vechten and Phillips.[20] The Pauling radii are larger for the cations but smaller (in a similar amount) for the anions. However, the difference has a trivial effect on the CTB equations since a transformation $r_A \rightarrow r_A+\gamma$ and $r_C \rightarrow r_C-\gamma$ leaves the equations invariant.[16] This model gives good agreement for the II-IV-V_2 compounds (as noted by Abrahams and Bernstein)[17] when the column-IV atom is Si or Ge. The lattice parameters for some Ge compounds calculated from the ''CTB plus $\eta=\eta_{tet}$'' rule listed in Table I, are very close to the experimental values, with differences that are less than 1% for a, and less than 2% for η in all the semiconductors listed.

TABLE I. The model calculated a and c/a based on ''CTB $+\eta=\eta_{tet}$'' are compared with experimental values. The tetrahedral radii of Zn, Cd, Ge, As, P are taken from Pauling's work. R_{Mn} is calculated from the bond length of MnS, MnSe, and MnTe, where the radii of S, Se, and Te are also taken from Pauling's work. The experimental values are cited from Ref. 16 and references therein.

Compound	a		c/a	
	Calc. (Å)	Expt. (Å)	Calc.	Expt.
$ZnGeP_2$	5.510	5.465	1.945	1.958
$ZnGeAs_2$	5.695	5.672	1.946	1.966
$CdGeP_2$	5.780	5.740	1.854	1.877
$CdGeAs_2$	5.966	5.945	1.858	1.886
$MnGeP_2$	5.673		1.889	
$MnGeAs_2$	5.858		1.892	

We interpolated a and c/a for $Cd_{1-x}Mn_xGeP_2$ from the experimental values for $CdGeP_2$ and the ''CTB plus $\eta=\eta_{tet}$'' value of $MnGeP_2$. This approximation is equivalent to Vegards' law, and works well in this system. For instance, it is reported that the lattice constant decreases to 5.695 Å when the Mn concentration becomes greater than Cd, which means x in the range of 50% to 53% since the maximum x is 53% in the experiment. Our interpolated lattice constant for $x=0.5$ is 5.706 Å, which is different from experiment by only 0.4%.

The DMOL^3 calculated structural parameters for $CdGeP_2$ listed in Table II show that the LDA functional predicts a very good lattice constant a, and the distortion of the zinc-blende structure, η. Although the GGA functional gives a

TABLE II. DMOL^3 calculated structural parameters of $CdGeP_2$ in comparison with experimental values.

	a (Å)	c/a	u
Expt.	5.74	1.877	0.283
LDA	5.71	1.882	0.279
GGA	5.84	1.887	0.282

TABLE III. Bond length (in Å) of Mn-P in the DMOL^3 optimized $Cd_{1-x}Mn_xGeP_2$ structure.

	FM2			AFM		
x	0.25	0.5	1.0	0.25	0.5	1.0
LDA	2.420	2.426	2.332	2.420	2.390	2.408
GGA	2.430	2.441	2.440	2.430	2.434	2.428

1.7% overestimate for a, it predicts a better internal structural parameter u (0.282) which is very close to experiment. This gives us confidence in optimizing the internal structural parameters in $Cd_{1-x}Mn_xGeP_2$ with GGA functionals. As an extensive test, calculations with LDA functionals were also done for $Cd_{1-x}Mn_xGeP_2$.

The internal structural parameters of $Cd_{1-x}Mn_xGeP_2$ were optimized by DMOL^3 until forces on atoms are less than 10^{-3} Htr/Bohr for both LDA and GGA. We found that the forces obtained from FLAPW calculations, which are based on the corresponding DMOL^3 optimized structures, are less than 2×10^{-3} and 5×10^{-3} Htr/Bohr for LDA and GGA, respectively. This indicates that the DMOL^3 optimization is in quite good agreement with FLAPW. The main relaxation comes from the P atoms, particularly those close to Mn, while Cd, Ge, and Mn atoms remain almost in the ideal lattice positions. The Mn-P bond lengths are listed in Table III. For $x=1.0$, the internal structure could be described by one parameter, u, as in pure $CdGeP_2$. The GGA FM gives a Mn-P bond length of 2.440 Å, which is equivalent to $u=0.258$. However, the description of the internal structures for $x=0.25$ and 0.50 becomes more complex since the P position changes not only in the [100] direction. In comparison with ideal $CdGeP_2$, the P atoms move closer to Mn atoms, which may be understood from the fact that the tetrahedral radius of Mn is smaller than that of Cd. Both LDA and GGA give close Mn-P bond lengths, around 2.43 Å, for different x except for $x=1.0$ with LDA.

The Mn-P bond length estimated under the CTB rule, i.e., the sum of Mn and P tetrahedral radii, 2.42 Å, is in very good agreement with the first-principles calculations. This means that the lattice constants obtained from the ''CTB plus $\eta=\eta_{tet}$'' rule and the interpolated values are quite reasonable. As expected, GGA gives a larger Mn-P bond length than LDA in corresponding systems, especially for $x=1.0$. According to our discussion on LDA and GGA effects in MnAs,[15] the GGA results for $x=1.0$ are more reliable. The good performance of the ''CTB plus $\eta=\eta_{tet}$'' rule enables us to carry out rapid investigations in the extensive exploration of materials with desired properties.

The energy differences between the AFM and FM states are listed in Table IV. The AFM configuration is described as a superlattice with period p and layer orientation **G** in Table IV. It is found that for $x=1.0$, the AFM state in $Cd_{1-x}Mn_xGeP_2$ is much lower in energy than the FM state, where both FLAPW and DMOL^3 give ΔE around -250 meV within GGA. For $x=0.5$ and 0.25, the value of ΔE dropped down to -20 ~-35 meV, with the AFM state still more stable than the FM state. The ΔE from LDA is similar to that of GGA for $x=0.25$ and 0.50, although it is around -160 meV for $x=1.0$, i.e., much smaller than that from GGA. The small energy difference between AFM and FM for $x=0.25$ and 0.5 suggests that the localized spin moments are weakly coupled. Clearly, both methods with different functionals predict that the AFM state is lower in energy for all x, which gives solid theoretical evidence that $Cd_{1-x}Mn_xGeP_2$ prefers AFM rather than FM ordering. This is not in agreement with the experimental result, which was interpreted as it behaving like a room-temperature ferromagnet.

TABLE IV. The energy difference between FM and AFM $Cd_{1-x}Mn_xGeP_2$ for $x=0.25$, 0.5, and 1.0.

x	p	**G**	$\Delta E=E_{AFM}-E_{FM}$ (meV/Mn) DMOL^3		FLAPW	
			LDA	GGA	LDA	GGA
0.25	1	(100)	-35	-21	-40	-30
0.50	1	(001)	-22	-35	-31	-35
1.00	1	(001)	-165	-258	-159	-248

The total spin moment of FM $Cd_{1-x}Mn_xGeP_2$ is $5.0\mu_B$ per Mn atom for $x=0.25$ within both LDA and GGA, and close to $5.0\mu_B$ for $x=0.50$. For $x=1.0$, it is still around $4.5\mu_B$ with GGA, but is reduced to $3.2\mu_B$ with LDA. It is easy to understand that the spin moment for $Cd_{1-x}Mn_xGeP_2$ is close to $5.0\mu_B$ per Mn since Mn substitutes Cd, a +2 cation. The reduced value for $x=1.0$ with LDA can be explained from the Mn-P bond lengths in Table III. The Mn-P bond length of FM $Cd_{1-x}Mn_xGeP_2$ for $x=1.0$ within LDA is obviously smaller than that in other Mn concentrations, which makes the interaction of Mn and P much stronger and reduces the Mn local moment. The big difference in ΔE between LDA and GGA for $x=1.0$ results from their different Mn moments in the FM states. Basically, the principal difference in magnetic properties between LDA and GGA results is due to their different predicted structures.

Unlike the Mn doped III-V semiconductors,[21] the Mn-induced FM moment at the anions gives positive contributions in $Cd_{1-x}Mn_xGeP_2$. As an example, the spin densities of FM and AFM $Cd_{1-x}Mn_xGeP_2$ for $x=0.5$ are shown in Fig. 1. Obviously, the positive spin density fills the bond area except for a small zone between Mn and P. The FM interaction between Mn and P seems to be a repulsive effect for the Mn-P bond since the FM Mn-P bond lengths are greater than those of AFM, as listed in Table III, and so increases the total energy of FM $Cd_{1-x}Mn_xGeP_2$. Mn-induced positive moments also exist at nearby Cd (not shown in Fig. 1) and Ge atoms. In the AFM state, the total P spin moment is close to zero.

The reason for the disagreement between our first-principles result and the experimental result[5] is not clear. In our calculations, $Cd_{1-x}Mn_xGeP_2$ is an ideal periodic bulk structure, while in experiment it is a surface-doped system with Mn concentration that decays from the surface to bulk. Clearly, the combined state-of-the-art FLAPW and DMOL^3 studies give solid evidence that the $Cd_{1-x}Mn_xGeP_2$ is an AFM system. To resolve the discrepancy between the experi-

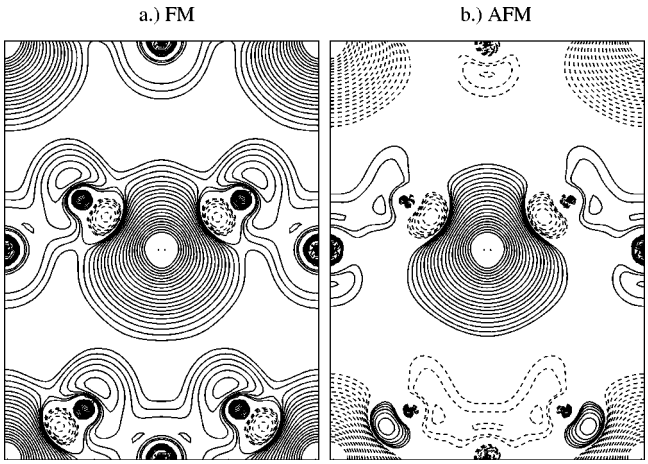

FIG. 1. Spin density of $Cd_{1-x}Mn_xGeP_2$ for $x=0.50$ from FLAPW calculations, plotted in the (110) plane. Spin density contours start at $5\times10^{-4}e$/a.u.^{3} and increase successively by a factor of $\sqrt{2}$. Positive spin density is represented by solid lines, while negative spin density is represented by dashed lines.

ment and our theoretical results, it is necessary to undertake more experiments on $Cd_{1-x}Mn_xGeP_2$, including careful characterizations.

Finally, some discussion about the energy gap in $Cd_{1-x}Mn_xGeP_2$ is called for. The energy gaps obtained from DMOL^3 calculations are listed in Table V. For $CdGeP_2$, LDA and GGA give 0.70 and 0.93 eV, respectively, which is 50% or more underestimated in comparison with the experimental value, 1.83 eV,[5] and is a well-known general tendency of LDA and GGA. In the AFM state, the energy gap decreases to 0.49 eV as the Mn composition x goes up to 0.50, although it increases to 0.71 eV as x goes to 1.0. In all cases, the energy gap of Mn-doped $CdGeP_2$ does not exceed that of pure $CdGeP_2$. In the FM state, there is no energy gap except for $x=0.25$. Therefore, the effect of Mn doping on the energy gap in $CdGeP_2$ is similar to that in the (Ga,Mn)As system, where it reduces the energy gap of the host semiconductor,[21] which disagrees with the report[5] of an energy gap increase upon Mn incorporation in $CdGeP_2$.

TABLE V. The energy gap in FM and AFM $Cd_{1-x}Mn_xGeP_2$ obtained from DMOL^3 calculation for $x=0$, 0.25, 0.5, and 1.0.

x	Energy gap (eV)			
	FM		AFM (Para for $x=0$)	
	LDA	GGA	LDA	GGA
0			0.70	0.93
0.25	0.0	0.16	0.31	0.58
0.50				0.49
1.00			0.37	0.71

Work supported by the NSF (through the Materials Research Center at Northwestern University).

[1] H. Ohno, A. Shen, F. Matsukura, A. Oiwa, A. Endo, S. Katsumoto, and Y. Iye, Appl. Phys. Lett. **69**, 363 (1996).
[2] H. Ohno, Science **281**, 951 (1998).
[3] Y. Ohno, D. K. Young, B. Beschoten, F. Matsukura, H. Ohno, and D. D. Awschalom, Nature (London) **402**, 790 (1999).
[4] H. Ohno, J. Magn. Magn. Mater. **200**, 110 (1999).
[5] G. A. Medvedkin, T. Ishibashi, T. Nishi, K. Hayata, Y. Hasegawa, and K. Sato, Jpn. J. Appl. Phys., Part 2 **39**, L949 (2000).
[6] E. Wimmer, H. Krakauer, M. Weinert, and A. J. Freeman, Phys. Rev. B **24**, 864 (1981), and references therein.
[7] B. Delley, J. Chem. Phys. **113**, 7756 (2000).
[8] B. Delley, J. Chem. Phys. **92**, 508 (1990).
[9] W. T. Geng, Yu-Jun Zhao, A. J. Freeman, and B. Delley, Phys. Rev. B **63**, 060101 (2001).
[10] B. Delley, Int. J. Quantum Chem. **69**, 423 (1998).
[11] S. H. Vosko, L. Wilk, and M. Nusair, Can. J. Phys. **58**, 1200 (1980); J. P. Perdew and Y. Wang, Phys. Rev. B **45**, 13 244 (1992).
[12] J. P. Perdew, K. Burke, and M. Ernzerhof, Phys. Rev. Lett. **77**, 3865 (1996).
[13] L. Hedin and B. I. Lundqvist, J. Phys. C **4**, 2064 (1971).
[14] G. A. Medvedkin, T. Ishibashi, T. Nishi, and K. Sato, Semiconductors **35**, 291 (2001).
[15] Yu-Jun Zhao, W. T. Geng, A. J. Freeman, and B. Delley (unpublished).
[16] J. E. Jaffe and A. Zunger, Phys. Rev. B **29**, 1882 (1984).
[17] S. C. Abrahams and J. L. Bernstein, J. Chem. Phys. **59**, 5415 (1973).
[18] D. R. Yoder-Short, U. Debska, and J. K. Furdyna, J. Appl. Phys. **58**, 4056 (1985).
[19] L. Pauling, *The Nature of the Chemical Bond* (Cornell University Press, Ithaca, New York, 1967).
[20] J. A. van Vechten and J. C. Phillips, Phys. Rev. B **2**, 2160 (1970).
[21] Yu-Jun Zhao, W. T. Geng, K. T. Park and, A. J. Freeman, Phys. Rev. B (to be published).